

Basolateral carbonic anhydrase IV in the proximal tubule is a glycosylphosphatidylinositol-anchored protein

JM Purkerson¹, AM Kittelberger¹ and GJ Schwartz¹

¹Department of Pediatrics, Strong Children's Research Center, University of Rochester School of Medicine, Rochester, New York, USA

Carbonic anhydrase (CA) IV facilitates HCO₃ reabsorption in the renal proximal tubule by catalyzing the reversible hydration of CO₂. CAIV is tethered to cell membranes via a glycosylphosphatidylinositol (GPI) lipid anchor. As there is basolateral as well as apical CAIV staining in proximal tubule, the molecular identity of basolateral CAIV was examined. Biotinylation of confluent monolayers of rat inner medullary collecting duct cells stably transfected with rabbit CAIV showed apical and basolateral CAIV, and in the cell transfectants expressing high levels of CAIV, a transmembrane form was targeted to the basolateral membrane. Basolateral expression of CAIV (~46 kDa) was confirmed in normal kidney tissue by Western blotting of vesicle fractions enriched for basolateral membranes by Percoll density fractionation. We examined the mode of membrane linkage of basolaterally expressed CAIV in the kidney cortex. CAIV detected in basolateral or apical membrane vesicles exhibited similar molecular size by sodium dodecyl sulfate (SDS)-polyacrylamide gel electrophoresis following deglycosylation, and was equally sensitive to phosphatidylinositol-specific phospholipase C digestion, indicating that CAIV is expressed on the basolateral membrane as a GPI-anchored protein. Half of the hydratase activity of basolateral vesicles was resistant to SDS denaturation, compatible with being CAIV. Thus, GPI-anchored CAIV resides in the basolateral membrane of proximal tubule epithelia where it may facilitate HCO₃ reabsorption via association with kNBC1.

Kidney International (2007) **71**, 407–416. doi:10.1038/sj.ki.5002071; published online 17 January 2007

KEYWORDS: membrane vesicles; Western blot; immunohistochemistry; Percoll density fractionation; rabbit kidney

Correspondence: GJ Schwartz, Department of Pediatrics, Strong Children's Research Center, University of Rochester School of Medicine, Rochester, New York, USA. E-mail: george_schwartz@urmc.rochester.edu

Received 3 June 2006; revised 22 October 2006; accepted 7 November 2006; published online 17 January 2007

Carbonic anhydrases (CAs) facilitate renal acidification in the kidney by catalyzing the hydration of CO₂ or the reverse reaction, the dehydration of bicarbonate.¹ The majority of the CA activity in the kidney (~95%) is comprised of cytosolic CAII.¹ CAIV is one of three membrane-associated CA isoforms,² the others being CAXII^{3–7} and in rodent species, CAXIV,^{8,9} that account for the remaining CA activity in the kidney. In humans, rabbits, and rodent species CAIV is expressed in the proximal tubule (S2 > S1 ≫ S3) and in distal nephron segments including outer and inner medullary collecting ducts (IMCDs) and α -intercalated cells of the cortical collecting duct.¹ A major role for CAIV in urinary acidification has been demonstrated in studies where inhibition of luminal CA activity eliminates nearly all net bicarbonate reabsorption in the proximal tubule¹⁰ and outer medullary collecting duct from the inner stripe,¹¹ and in CAII-deficient patients and mice where inhibition of CA activity diminishes renal acid secretion.^{12,13}

CAIV is unique among CA isoforms, because it is tethered to the plasma membrane via a glycosylphosphatidylinositol lipid anchor (GPI-anchor).^{14,15} Most GPI-anchored proteins are targeted to the apical membrane of polarized epithelial cells;¹⁶ nevertheless, CAIV immunoreactivity detected with different CAIV antibodies has been observed on the basolateral membranes of proximal tubule segments in human, rabbit and rodent species.^{2,17,18} Studies from our laboratory have functionally demonstrated in the proximal tubule the existence of a basolateral CA activity that facilitates fluid and bicarbonate absorption.¹⁹ These studies suggested that either a transmembrane form is expressed basolaterally or perhaps that GPI-anchored CAIV is additionally targeted to the basolateral membrane. However, with the recent description of CAXII as a major CA isoform that is expressed on the basolateral membranes of acidifying nephron segments,⁴ the molecular identity of the basolaterally expressed CA detected by anti-CAIV antibodies required investigation.

In this study, we characterized the polarity and the molecular form of CAIV immunoreactivity in rabbit kidney cortex and in transfected renal IMCD epithelial cells in culture. Whereas in IMCD cells overexpressing CAIV, a transmembrane form is preferentially expressed on the

basolateral membrane, we found that CAIV is normally expressed on both the apical and basolateral membranes of proximal tubule epithelial cells as a GPI-anchored protein.

RESULTS

Trafficking to the basolateral membrane is an intrinsic property of the CAIV molecule

CAIV is tethered to cell membranes via a GPI anchor, and typically GPI-anchored proteins are targeted to the apical membrane of polarized epithelial cells. However, as shown in Figure 1, immunohistochemical staining of kidney cortex with antibodies to CAIV consistently showed basolateral staining of proximal tubules in addition to apical labeling.

The following experiments were designed to determine whether trafficking to the basolateral membrane of renal epithelial cells is an intrinsic property of the CAIV molecule, as well as to ascertain the molecular form of CAIV that is expressed basolaterally. In initial studies the polarity of CAIV expression in an *in vitro* culture model of polarized renal epithelial cells was examined. IMCD cells were selected for these studies owing to their ability to form confluent monolayers with high transepithelial resistance. Confluent monolayers of IMCD cells stably transfected with a full-length CAIV exhibiting transepithelial resistance in the range of 900–1500 Ωcm^2 were subjected to apical and basolateral surface biotinylation. Biotinylated proteins were precipitated with streptavidin (SAv)-agarose and levels of CAIV and apically (GP135) or basolaterally (Na^+ , K^+ -ATPase) expressed proteins were determined by Western blotting. The results of three independent biotinylation experiments are shown in Figure 2a, where GP135 was precipitated predominantly from cells biotinylated on the apical surface and Na^+ , K^+ -ATPase was exclusively precipitated from cells biotinylated on the basolateral side, demonstrating the specificity of apical versus basolateral surface biotinylation. CAIV, on the other hand, was equally precipitated from cells

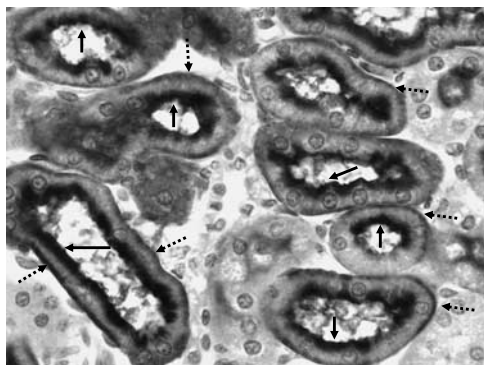


Figure 1 | CAIV immunoreactivity is observed on the apical and basolateral membrane of proximal tubules. Paraffin-embedded sections of rabbit kidney were stained with a goat anti-rabbit CAIV antibody (YDQR). The slide was developed with an HRP-conjugated anti-goat antibody utilizing the DAB substrate and counterstained with hematoxylin. Solid arrows indicate apical staining, whereas dashed arrows point to basolateral staining. Original magnification $\times 100$.

biotinylated on either the apical or basolateral side. These results demonstrated that CAIV was sorted to both apical and basolateral membranes of polarized renal epithelial cells.

Because GPI-anchor attachment results in apical sorting of many proteins in polarized epithelial cells, we examined whether expression of a transmembrane form of CAIV explained basolateral expression of CAIV in transfected IMCD cells. CAIV was subcloned into the pcDNA 3.1 vector (see Figure 2b), so that CAIV expressed as a transmembrane protein would contain a 6XHis epitope-tag contiguous with

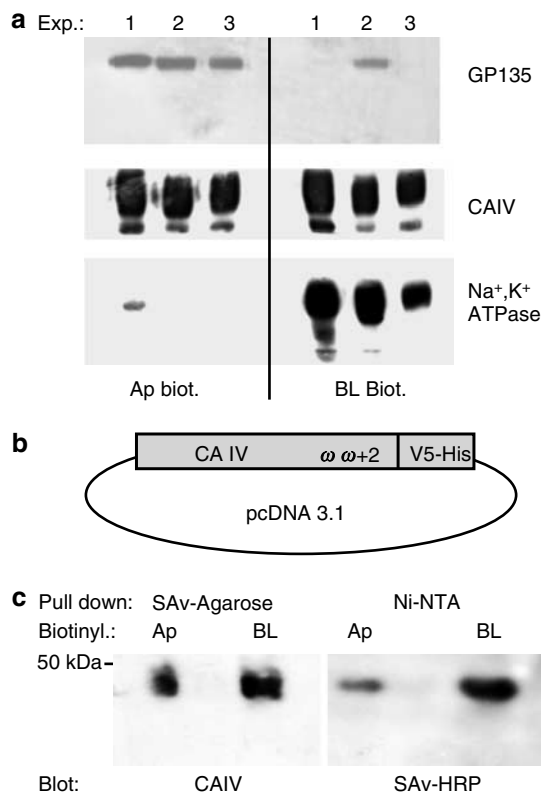


Figure 2 | CAIV is expressed on the apical and basolateral membranes of IMCD transfectants. (a) Confluent monolayers of IMCD cells stably transfected with rabbit CAIV were grown on Transwell[®] permeable supports and surface biotinylated on either the apical or basolateral side. Biotinylated proteins were precipitated from cell lysates with SAv-agarose. Levels of SAv-precipitated apical (GP135), basolateral (Na^+ , K^+ -ATPase) proteins, and CAIV were determined by Western blotting. Results of three independent surface biotinylation experiments are shown. (b) Rabbit CAIV was subcloned into the pcDNA 3.1 vector so that CAIV expressed as a transmembrane protein containing the V5-6X His epitope tags. Omega (ω) and ($\omega + 2$) denote the serine residue at which GPI-anchor attachment occurs and the amino-acid residue that plays a key role in the efficiency of lipid anchor linkage, respectively. (c) Confluent monolayers of IMCD cells stably transfected with rabbit CAIV-pcDNA 3.1 construct were surface biotinylated on the apical or basolateral side. Biotinylated proteins were precipitated from cell lysates with SAv-agarose or V5-His-tagged proteins with Ni-NTA-agarose. Levels of transfected CAIV precipitated by Ni-NTA-agarose were determined by blotting with SAv-HRP, whereas GPI-linked CAIV precipitated with SAv-agarose was determined by blotting with anti-rabbit CAIV (KDNV). Results presented in (c) are representative of two independent experiments.

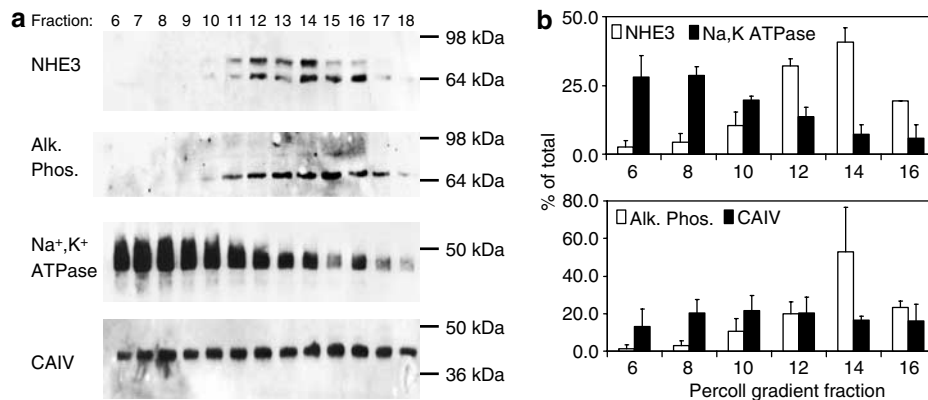


Figure 3 | Anti-CAIV antibodies detect a 46 kDa protein in both apical and basolateral membrane vesicles. Membrane vesicles prepared from kidney cortex were fractionated on a Percoll density gradient. Expression of apical (NHE3, alkaline phosphatase) and basolateral (Na⁺,K⁺-ATPase) membrane proteins and CAIV in the indicated Percoll gradient fractions was determined by Western blotting. (a) Immunoblots of membrane vesicle fractions containing 25 μg (NHE3), 60 μg (alkaline phosphatase), 0.5 μg (Na⁺,K⁺-ATPase), and 5 μg (CAIV) of total protein. (b) Percentage of total NHE3, alkaline phosphatase, Na⁺,K⁺-ATPase, and CAIV in each Percoll gradient fraction determined from densitometric scans of four independent experiments. The percentage of total for the respective proteins was determined by dividing the band intensity for each fraction by the summation of band intensity for all fractions (× 100).

the COOH-terminal tail region.²⁰ Confluent monolayers (transepithelial cell resistance ranging from 800 to 1000 Ωcm²) of IMCD cells stably transfected with CAIV-pcDNA 3.1 were subjected to surface biotinylation on either the apical or basolateral side. In the experiment shown in Figure 2c biotinylated proteins were either precipitated from solubilized membranes with SAV-agarose and precipitated CAIV was detected with anti-CAIV antibody by Western blotting, or alternatively a putative transmembrane form of CAIV (His-tagged CAIV) was precipitated with Ni-nitrilotriacetic acid (NTA)-agarose and subsequently detected by blotting with SAV conjugated to horseradish peroxidase (SAV-HRP). Consistent with the experiment shown in Figure 2a, SAV-agarose precipitated CAIV from membranes subjected to either apical or basolateral surface biotinylation, indicating that CAIV was expressed on both membranes. In contrast, precipitation of a transmembrane form of CAIV with Ni-NTA occurred predominantly from membranes that had been biotinylated on the basolateral side. Results presented in Figure 2c are representative of two independent experiments and indicate that under conditions of high-level expression in polarized renal epithelial cells, a portion of CAIV produced is expressed as a transmembrane protein, and the non-GPI-linked form of CAIV is preferentially targeted to the basolateral membrane.

Antibodies to CAIV detect a 46 kDa protein in both apical and basolateral membranes from kidney cortex

The identity of CAIV immunoreactivity on the basolateral membrane of renal proximal tubules was examined by enrichment of basolateral membranes via Percoll density fractionation of membrane vesicles prepared from kidney cortex. The levels of apical (NHE3) and basolateral (Na⁺,K⁺-ATPase) proteins, as well as GPI-anchored proteins (CAIV and alkaline phosphatase) in Percoll gradient

fractions were quantified by Western blotting. As shown in Figure 3a, fractions 6–10 were enriched for basolateral membranes, as they contained abundant levels of Na⁺,K⁺-ATPase, whereas NHE3 was undetectable. Fractions 11–17 contained NHE3 and alkaline phosphatase and exhibited declining levels of Na⁺,K⁺-ATPase, indicating that these latter fractions were enriched for apical membrane vesicles. Antibodies to rabbit CAIV that do not crossreact with CAXII⁶ detected a 46 kDa protein across the entire Percoll density gradient, including fractions enriched for basolateral membrane vesicles (6–10); thus, CAIV was present in both apical and basolateral membrane vesicles. This contrasted with another GPI-anchored protein, alkaline phosphatase, which clearly exhibited a distribution consistent with apical expression (Fr. 11–17). Figure 3b shows the average and s.d. of four independent membrane vesicle fractionations presented as the percentage of the respective protein total in each Percoll fraction. Note that alkaline phosphatase co-distributed with NHE3, whereas CAIV was consistently detected in basolateral membrane fractions (below 10), characterized by abundant levels of Na⁺,K⁺-ATPase and low or undetectable levels of NHE3 and alkaline phosphatase. CAIV in basolateral membrane fractions (below 10) comprised 31.1 ± 12.3% of the total CAIV content of the Percoll density gradients. These results confirm that CAIV is expressed on basolateral membranes of the renal proximal tubule.

CAIV expressed on apical and basolateral membranes is equally sensitive to cleavage by PI-PLC

To determine whether CAIV is expressed as a GPI-anchored protein in proximal tubule epithelia, CAIV sensitivity to cleavage by phosphatidylinositol-specific phospholipase C (PI-PLC) was examined. In initial studies total membranes prepared from kidney cortex were subjected to PI-PLC digestion for 1–4 h, and GPI-anchored protein was

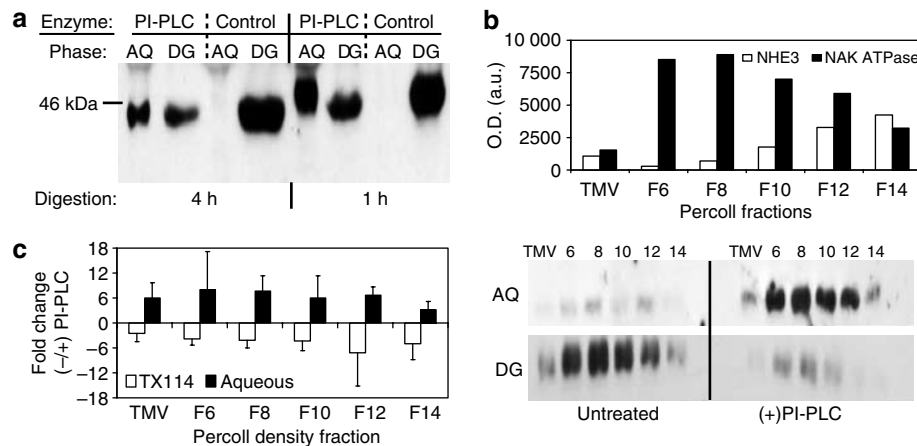


Figure 4 | CAIV expressed on the apical and basolateral membranes of the proximal tubule are both sensitive to cleavage by PI-PLC. (a) Membranes (25 μ g total protein) prepared from kidney cortex were digested with 500 mU PI-PLC for 1–4 h. GPI-linked/transmembrane proteins were phase separated from enzymatically cleaved CAIV by extraction with Triton X-114. AQ = aqueous phase; DG = Triton X-114 phase DG. (b) The levels of NHE3 and Na⁺,K⁺-ATPase in membrane vesicle fractions determined by Western blotting are shown as a plot of densitometric scans of film exposures to luminescence. Membrane vesicle fractions were treated with PI-PLC as described or left untreated (see Materials and Methods) and GPI-anchored/transmembrane proteins were separated from non-GPI-linked protein by Triton X-114 extraction as in (a). Lower portion of this panel shows levels of CAIV in the AQ and DGs of control and PI-PLC-treated fractions determined by Western blotting with anti-rabbit CAIV (YDQR). (c) The results of three additional independent experiments are presented as the mean and s.d. of the fold increase and decrease of CAIV in AQ and DGs, respectively, following PI-PLC digestion and extraction with Triton X-114. The changes in CAIV partitioning induced by PI-PLC were not significantly different between fractions 6 and 8 and 10 and 12 as determined by two-tailed, Student's *t*-test, assuming equal variance (fold change in AQ $P > 0.31$, DG $P > 0.38$).

partitioned from cleaved CAIV by extraction with Triton X-114. Figure 4a shows the result of one such experiment in which the levels of GPI-anchored CAIV in the detergent phase (DG) and cleaved CAIV in the aqueous phase (AQ) were determined by Western blotting. In the absence of PI-PLC digestion most of the CAIV partitions into the DG ($89 \pm 10\%$, $n = 7$). It is important to note that Triton X-114 partitioning does not distinguish between transmembrane and GPI-anchored forms of CAIV, because transmembrane as well as GPI-anchored proteins partition into the DG. Following PI-PLC digestion most, but not all, of the CAIV partitions into the AQ ($67 \pm 14\%$, $n = 7$), indicative of removal of the GPI anchor. Despite increasing the length of PI-PLC digestion from 1–4 h, partitioning of CAIV into the AQ never approached 100%. Incomplete release of GPI-anchored proteins from membranes following PI-PLC treatment is not uncommon,²¹ and possible explanations include sequestration into membrane invaginations, localization in a lipid environment that prevents PI-PLC access, the presence of inside-out vesicles, or attachment of CAIV by a GPI isoform that is resistant to cleavage.

Whether or not the PI-PLC insensitive pool ($\sim 30\%$) comprised basolateral membrane resident CAIV was examined by quantifying the PI-PLC sensitivity of CAIV in Percoll-fractionated membrane vesicles. In the experiment shown in Figure 4b, total membrane vesicles, basolateral membrane-enriched fractions (Fr. 6 and 8), or fractions containing increasing amount of apical vesicles (Fr. 10–14), were subjected to extensive PI-PLC digestion or left untreated. Cleaved CAIV was separated from the GPI-anchored protein

by Triton X-114 partitioning. As noted above, in the absence of PI-PLC digestion CAIV in membrane vesicle fractions partitioned into the DG phase, whereas PI-PLC treatment resulted in increased partitioning to the AQ from all membrane vesicle fractions including fractions enriched from basolateral membranes (Fr. 6 and 8). Figure 4c shows the summary of four independent experiments presented as the fold decrease in partitioning to the DG along with the fold increase AQ partitioning following PI-PLC digestion. The decrease in DG CAIV upon PI-PLC digestion in basolateral fractions 6 and 8 was not significantly different from that observed in apical fractions (12 and 14; $P > 0.39$). Similarly, the PI-PLC induced increase in AQ CAIV in basolateral fractions was not different from apical fractions ($P > 0.32$). These data demonstrate that CAIV is expressed on the apical and basolateral membranes of the proximal tubule as a GPI-anchored protein. And as CAXII is not a GPI-anchored protein, cleavage by PI-PLC provides additional evidence that the basolaterally expressed protein that was detected by anti-CAIV antibodies is not CAXII.

CAIV is expressed in the kidney cortex as a single molecular weight species

GPI-anchor attachment occurs at serine residue 280 of CAIV and results in the removal of 28 amino acids (MW = 2870.1) from the COOH-terminal tail. If CAIV were expressed as both a GPI-anchored and a transmembrane protein, then two molecular species of CAIV differing by ~ 3 kDa should exist in renal epithelial cells.²⁰ To confirm that CAIV is expressed only as a GPI-anchored protein in the proximal tubule, the

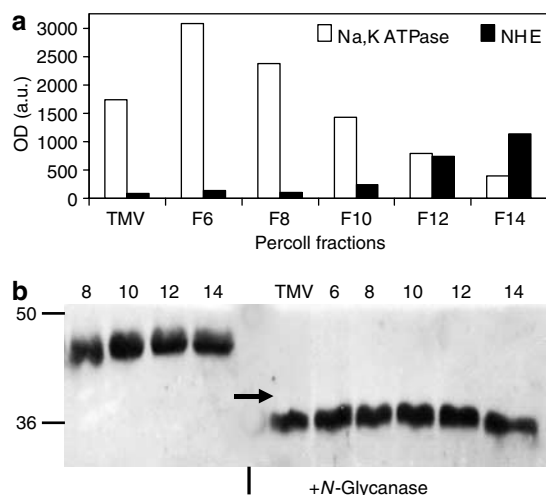


Figure 5 | CAIV is expressed as a single molecular weight species in kidney cortex. (a) levels of NHE3 and Na^+, K^+ -ATPase in the indicated Percoll density fractions as determined by Western blotting. Results presented are optical density values generated by densitometric scans of film exposed to luminescence. (b) fractionated membrane vesicles were treated with *N*-glycanase F or left untreated and then resolved by SDS-PAGE. The arrow indicates the calculated position of a putative transmembrane form of CAIV.

molecular weight of CAIV peptides in membrane vesicle fractions isolated from rabbit kidney cortex was examined following removal of N-linked sugars by treatment with *N*-glycanase. As shown in Figure 5, in the absence of deglycosylation CAIV exhibits an apparent molecular weight of ~ 46 kDa as determined by sodium dodecyl sulfate-polyacrylamide gel electrophoresis (SDS-PAGE). Treatment of membrane vesicle fractions with *N*-glycanase reduces the apparent molecular weight by about 10 kDa, demonstrating that in contrast to CAIV in human tissue, CAIV is heavily glycosylated in the rabbit. All of the membrane vesicle fractions, including total membrane vesicles, contained a single molecular weight species of deglycosylated CAIV. Furthermore, there was no apparent difference in the molecular weight (~ 35 – 36 kDa) of deglycosylated CAIV from basolaterally enriched fractions (Fr. 6 and 8) compared to fractions containing apical membrane vesicles (Fr. 10–14). These findings provide additional support for the conclusion that CAIV is expressed as a GPI-anchored protein on the basolateral membrane of the proximal tubule. And because CAXII exhibits a predicted molecular weight of ~ 40 kDa, it is evident that CAXII is not detected by our antibody against rabbit CAIV.

CAIV accounts for approximately half of the CA activity in basolateral membrane of the rabbit proximal tubule

CAXII is another CA isoform that is expressed basolaterally in the proximal tubule.⁴ Accordingly, we sought to determine the extent to which CAIV contributes to hydratase activity in basolateral membrane vesicles. Owing to the presence of two disulfide bridges,²² CAIV is resistant to denaturation by

Table 1 | The effect of SDS treatment on hydratase activity in membrane fractions isolated from kidney cortex

Fraction	Exp. 1		Exp. 2		Exp. 3	
	Untreated	1% SDS	Untreated	1% SDS	Untreated	1% SDS
Ms CTX	91 ± 14	20 ± 8				
Rb CTX	40 ± 2	35 ± 7	47 ± 4	38 ± 3	49 ± 4	41 ± 3
Fr. 6	88 ± 5	52 ± 14	95 ± 8	50 ± 7	114 ± 2	54 ± 3
Fr. 8	85 ± 4	45 ± 3	65 ± 6	43 ± 3	89 ± 2	37 ± 4
Fr.10	91 ± 8	74 ± 9	92 ± 16	85 ± 16	101 ± 4	64 ± 12
Fr.16	85 ± 5	97 ± 11	77 ± 12	74 ± 5	88 ± 7	75 ± 9
Fr.18	57 ± 16	68 ± 17	64 ± 3	75 ± 7	76 ± 10	68 ± 16

SDS, sodium dodecyl sulfate.

Results presented are the mean \pm s.d. for triplicate assays of hydratase activity (EU/mg protein) determined using a microassay technique as described in Materials and Methods. 'Ms CTX' denotes a total membrane fraction prepared from mouse kidney cortex, whereas Rb CTX indicates total membrane vesicle preparations from rabbit kidney cortex before fractionation on Percoll density gradients. Fractions 6 and 8 (Fr. 6, 8) correspond to Percoll fractions enriched for basolateral membranes, Fr. 10 is an intermediate fraction, whereas fractions 16 and 18 are enriched for apical membranes (Figure 6a).

treatment with SDS (0.1–1%), whereas other CA isoforms expressed in the kidney (CAXII, CAII, and CAXIV in rodent species) are denatured by SDS treatment.^{6,23} Therefore, differential sensitivity to denaturation by SDS was used to assess the contribution of CAIV to CA hydratase activity in apical and basolateral membranes of the proximal tubule. CA hydratase activity in membrane preparations was measured by a microassay method, as described by Brion *et al.*^{24,25} SDS treatment of total membranes prepared from mouse kidney cortex reduced hydratase activity by 83%, indicating that CA isoforms other than CAIV (e.g. CAXII and CAXIV) account for the bulk of membrane-associated CA activity in mouse kidney (Table 1, Figure 6b). In contrast, 80–86% of the hydratase activity in total membrane vesicles isolated from rabbit kidney cortex was resistant to SDS treatment, in keeping with our previous study.²⁵ Thus, unlike the mouse, CAIV accounts for most (80–90%) of the membrane-associated CA hydratase activity in the rabbit kidney cortex.

To assess the contribution of CAIV to hydratase activity in apical and basolateral membranes of the proximal tubule, the microassay method was used to measure CA activity in vesicles enriched for basolateral or apical membranes by Percoll density fractionation. As shown in Figure 6a, fractions 6 and 8 contained CAIV-containing vesicles enriched for basolateral membranes, characterized by abundant Na^+, K^+ -ATPase, and virtually undetectable levels of NHE3. In three independent experiments, 40–60% of the hydratase activity in basolateral membranes (Fr. 6 and 8) was resistant to denaturation by SDS, indicating that CAIV accounts for approximately half of the CA hydratase activity in basolateral membranes from rabbit proximal tubule. In contrast, in apical membrane fractions (Fr. 16–18), characterized by abundant NHE3 and low level Na^+, K^+ -ATPase (Figure 6a), most of the hydratase activity (85–100%) was resistant to SDS (Table 1 and Figure 6b) (note in Table 1 that in those instances where mean hydratase activity was slightly higher in SDS-treated apical samples compared to untreated samples,

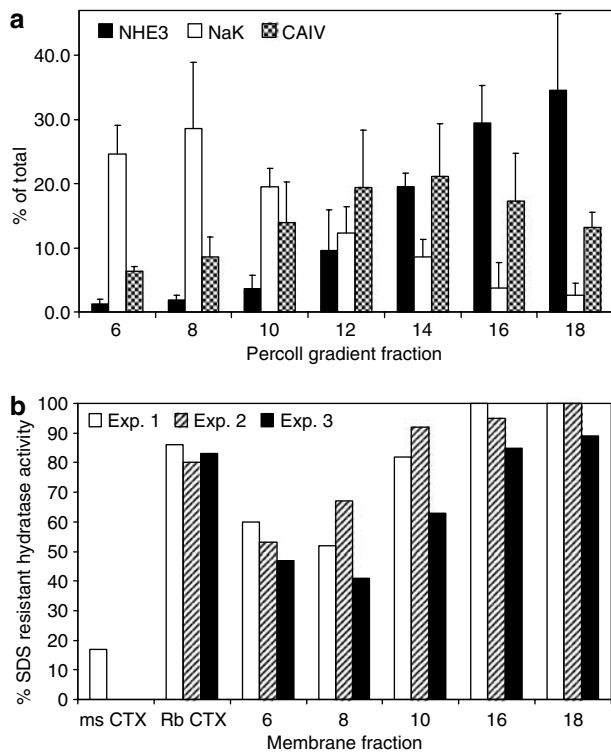


Figure 6 | CAIV contributes to hydratase activity of basolateral membrane vesicles. Membrane vesicles prepared from kidney cortex were fractionated on a Percoll density gradient. (a) Expression of apical (NHE3, alkaline phosphatase) and basolateral (Na^+/K^+ -ATPase) membrane proteins and CAIV in the indicated Percoll gradient fractions was determined by Western blotting and the percentage of total NHE3, Na^+/K^+ -ATPase, and CAIV in each Percoll gradient fraction determined from densitometric scans of three independent experiments. (b) The percentage of SDS-resistant hydratase activity (corresponding to CAIV) in total membranes isolated from mouse kidney cortex (Ms CTX), total membrane vesicles from rabbit kidney cortex (Rb CTX), and Percoll density fractions shown in (a).

the SDS-resistant activity was deemed to be 100% (Figure 6b). Slightly increased CA activity following SDS treatment was typically observed when boiled samples were used as a baseline control (Exp. 1 and 2). When acetazolamide-treated controls were used to establish baseline activity, SDS-resistant activity did not exceed 100% (Exp. 3). The latter result is consistent with the conclusion that CAIV is the only membrane CA isoform expressed apically in the proximal tubule. More importantly, these results indicate that both CAIV and CAXII contribute to basolateral hydratase activity that facilitates bicarbonate reabsorption in the rabbit proximal tubule.

DISCUSSION

The principal finding of this study showed that CAIV was expressed on both the apical and basolateral membranes of polarized renal proximal tubular epithelial cells as a GPI-anchored protein. We have confirmed (Figure 1) the results of immunohistochemical studies² by demonstrating that

proximal tubule basolateral membranes enriched from kidney cortex contain immunoreactivity that is identical in molecular weight to CAIV in apical membrane fractions (Figure 5). These results rule out the possibility that antibodies to CAIV were crossreacting with another CA isoform (e.g. CAXII) that is expressed in basolateral membranes of the proximal tubule. Approximately half of the basolateral hydratase activity was resistant to SDS denaturation (Figure 6), indicating that it was CAIV. Furthermore, the amount of CAIV in basolateral membrane fractions comprised a substantial portion (~30%) of the total CAIV protein, suggesting that levels of basolaterally expressed CAIV are sufficient for facilitation of acid/base transport in the proximal tubule, as shown in previous functional studies.¹⁹

In addition to CAIV reported herein, carboxypeptidase M and PrP^C are two other examples of GPI-anchored proteins that are either targeted to both apical and basolateral membranes (carboxypeptidase M)²⁶ or are preferentially sorted to basolateral membranes (PrP^C)²⁷ in MDCK cells. Interestingly, alkaline phosphatase and five other GPI-anchored proteins exhibited the expected apical localization.²⁶ In contrast, in another cell culture model, Fischer rat thyroid epithelial cells, six out of nine detectable endogenous GPI-anchored proteins were localized on the basolateral surface, two were apical and one was not polarized.²⁸ Accordingly, ours may be the first report demonstrating both apical and basolateral targeting of a GPI-anchored protein in polarized epithelial cells from normal tissue.

Studies utilizing a cell culture model confirmed that apical and basolateral targeting of CAIV is an intrinsic property of the CAIV molecule. CAIV was expressed on both apical and basolateral membranes in transfected IMCD cells (Figure 2a), a polarized renal epithelial cell line derived from the distal nephron.²⁹ In the IMCD-transfected model we also found that CAIV expressed as transmembrane protein was preferentially targeted to the basolateral membrane (Figure 2b). Basolateral targeting of the transmembrane form of CAIV is consistent with the presence of putative dileucine basolateral sorting motifs within the COOH-terminal tail of CAIV.^{20,30} However, CAIV expressed in basolateral and apical membranes from kidney cortex was equally sensitive to PI-PLC cleavage (Figure 4), as was shown by McGwire *et al.*²⁶ for carboxypeptidase M in MDCK cells, indicating that CAIV is expressed on both membranes as a GPI-anchored protein. Furthermore, we found no evidence for expression of a ~3 kDa higher-molecular weight species corresponding to a putative transmembrane form of CAIV in kidney cortex (Figure 5). Expression of a transmembrane CAIV in the IMCD transfectant was most likely due to exceptionally high CAIV expression level driven by the CMV promoter of the pcDNA 3.1 vector, which could have overloaded the capacity of either GPI-anchor attachment or the rate of transmembrane form degradation in the endoplasmic reticulum.^{31,32}

Expression of CAIV as a transmembrane protein has been observed in normal pancreatic ducts. Fanjul *et al.*³³ reported

that CAIV expressed on the luminal or apical surface of ductal cells was insensitive to PI-PLC cleavage and was detected by polyclonal antisera raised against the COOH terminal tail that is normally cleaved upon GPI-anchor attachment. Results of this study conflict with our findings in the IMCD transfectant model, where transmembrane CAIV was preferentially targeted to the basolateral membrane (Figure 2b). The functional significance of transmembrane CAIV is unclear, as cleavage of the COOH-terminal tail of CAIV has been reported to be necessary for realization of full enzyme activity.³⁴ Mutations of the ω site prevented removal of the C-terminal hydrophobic domain, such that the mutated CAIV was inactive, not GPI-anchored, and not expressed on the cell surface.³⁴

Overall, the results of our study suggest that CAIV has a strong proclivity for trafficking to the basolateral membrane of proximal tubular epithelial cells even in the context of GPI-anchor attachment. It is important to note, however, that in distal nephron segments CAIV expression is detected exclusively on the luminal or apical membrane.² Furthermore, CAIV expressed in the rabbit kidney medulla exhibits a distinct glycosylation pattern from CAIV expressed in kidney cortex.² Differences in the molecular forms and localization of CAIV in kidney and pancreas suggest that cell-specific post-translational modification and/or trafficking of CAIV occurs in different types of polarized epithelial cells.

Early studies of protein trafficking indicated that GPI anchor attachment targeted proteins to the apical membrane of polarized epithelial cells. It was proposed that apical sorting resulted from segregation of GPI-anchored proteins into membrane microdomains called lipid rafts or detergent-resistant membranes that are characterized by their lipid composition (e.g. enriched in cholesterol and sphingolipid content) and resistance to solubilization in non-ionic detergents such as Triton X-100.³⁵⁻⁴⁰ However, it is now clear that GPI-linkage and raft association alone is not sufficient for apical sorting. Several studies have dissociated apical sorting from raft association,^{27,41-43} and other sorting determinants such as *N*-glycans^{42,44} or oligomerization have been shown to exert a greater influence on apical targeting.^{45,46} Furthermore, trafficking of GPI-anchored proteins to the apical membrane can occur via either direct or indirect (transcytotic) pathways.^{41,47,48}

The extent to which *N*-glycans, protein oligomerization, or possibly other sorting determinants influence basolateral sorting of CAIV in the basolateral membrane has yet to be determined. It is interesting to speculate that CAIV trafficking via the indirect (transcytotic) pathway results in physical association with the sodium bicarbonate transporter, sodium bicarbonate co-transporter 1 (NBC1) and retention of CAIV in the basolateral membrane of the proximal tubule. NBC1 is abundantly expressed in the basolateral membrane of the proximal tubule where sodium-dependent co-transport results in bicarbonate and fluid reabsorption.⁴⁹ CAIV has been shown to associate with NBC1 to form the extracellular component of a bicarbonate transport meta-

bolon.⁵⁰ Previous studies from our laboratory have demonstrated the function of a basolateral, membrane-associated CA in bicarbonate and fluid reabsorption in the proximal tubule segments.¹⁹ Results of this study showing basolateral expression of CAIV in kidney cortex suggest that GPI-anchored CAIV may facilitate bicarbonate transport by NBC1 in the proximal tubule.

MATERIALS AND METHODS

Animals

New Zealand white rabbits were purchased from Hazelton-Dutchland farms (Denver, PA, USA) and maintained on a standard rabbit diet.² Adult rabbits (1.8–3.1 kg) were killed by intramuscular injection with xylazine (5 mg/kg) and ketamine (44 mg/kg) followed by an intracardiac injection of pentobarbital (100 mg/kg).

Reagents and antibodies

Recombinant PI-PLC from *Bacillus thuringiensis* expressed in *B. subtilis* and *N*-glycanase (peptide-*N*-glycosidase F; PNGase F; EC 3.5.1.52) isolated from *Escherichia coli* expressing a cloned gene from *Chryseobacterium (Flavobacterium) meningosepticum* were purchased from Prozyme (San Leandro, CA, USA). Polyclonal goat anti-rabbit CAIV peptide antibodies (KDNV and YDQR) were previously produced in our laboratory² and found not to crossreact with rabbit CAXII.⁶ Monoclonal anti- Na^+ , K^+ -ATPase α -1, clone C464.6 (Upstate Cell Signaling Solutions, Lake Placid, NY, USA), and anti-alkaline phosphatase, tissue nonspecific (ab17973, AbCam Inc., Cambridge, MA, USA) were used to identify basolateral and apical GPI-anchored proteins, respectively. Monoclonal anti-NHE3 (Clone MAB3134) raised against the rabbit Na^+ / H^+ exchanger 3 was purchased from Chemicon International, (Temecula, CA, USA). Monoclonal anti-GP135 antibody was a kind gift from Dr George Ojakian.⁵¹ HRP-conjugated secondary antibodies utilized in this study included donkey anti-mouse, -rabbit, or -goat obtained from Jackson ImmunoResearch, West Grove, PA, USA.

Immunohistochemical staining

Expression of CAIV in kidney sections was visualized by immunostaining as described previously.² Briefly, rabbit kidneys were perfusion fixed in periodate-lysine-paraformaldehyde or a non-formaldehyde-based fixative, Prefer (Anatech, Battle Creek, MI, USA). Kidney slices (1–2 mm) were then incubated overnight at 4°C in the same fixative used for perfusion fixation. Sections were then rinsed in 70% ethanol, embedded in paraffin, and 4 μm sections were collected on slides (Superfrost⁺, VWR Scientific, Piscataway, NY, USA). After deparaffinization and hydration, antigen retrieval was accomplished by heating slides in a microwave for 5 min in 1 mM ethylenediaminetetraacetic acid (EDTA), pH 8. Endogenous peroxidase was quenched by incubating slides in 0.3% H_2O_2 , and tissue was permeabilized by treatment with 0.3% Triton X-100 in TBS (tris-buffered saline). Slides with blocked with 10% horse serum-TBS, and goat anti-rabbit CAIV (YDQR) antibody was applied at a 1/125 dilution in 5% horse serum-TBS and incubated overnight at 4°C. Slides were developed by incubating with biotinylated horse anti-goat secondary (Vector, Burlingame, CA, USA) followed by avidin-biotinylated HRP (Vectastain Elite, Vector Labs, Inc., Burlingame, CA, USA) according to the manufacturer's recommended protocol. Slides were counter-stained with hematoxylin according to recommended protocols (Sigma Diagnostics[®], St Louis, MO, USA). Digital Images were produced using the Spot

RT color digital camera (Diagnostics Instruments Inc., Sterling Heights, MI, USA) mounted on an Olympus BX51 microscope ($\times 60$ brightfield, oil immersion) and the Spot Basic Image Software (Diagnostic Instruments).

IMCD transfectants

Rat IMCD cells²⁹ were grown in low-glucose Dulbecco's modified Eagle's medium supplemented with 10% fetal calf serum. 10 mM *N*-2-hydroxyethylpiperazine-*N'*-2-ethanesulphonic acid, 2 mM glutamine, penicillin G sodium (100 U/ml)-streptomycin sulfate (100 μ g/ml) (Invitrogen, Carlsbad, CA, USA). Full-length CAIV was cloned into the *Bam*HI-*Xho*I sites of pcDNA3 vector (Invitrogen). In order to facilitate analysis of the molecular form of CAIV expressed on the cell surface of IMCD cells, full-length CAIV was subcloned into the pcDNA3.1 directional Topo[®] Vector by polymerase chain reaction amplification (forward: ATGCAGC TACTGTTTGC; reverse: TCGGAGGAGGCC GGCCAT primers). The pcDNA3.1 vector contains V5 and 6XHis epitope tags contiguous with the CAIV sequence such that CAIV may be affinity isolated using Ni-NTA beads (see below). Expression vectors were transfected into IMCD cells utilizing either Lipofectamine[™] Reagent GIBCO/BRL[®] or DOTAP liposomal transfection reagent (ROCHE Diagnostics Corp. Indianapolis, IN, USA) according to the manufacturer's recommended protocols. Stable transfectants were generated by selection with 0.8–1 mg/ml G418 2 or 3 days post-transfection.

Biotinylation of apical versus basolateral membrane proteins

IMCD transfectants were seeded on polycarbonate Transwell[®] permeable supports (0.4 μ m pore size) at $10^6/4.67$ cm² or $10^7/44$ cm². The following day transepithelial resistance was measured with an EVOM[™] epithelial voltohmmeter (World Precision Instruments, Sarasota, FL, USA). Cells were washed ($3 \times$) with ice-cold Dulbecco's phosphate-buffered saline (Invitrogen). Apical biotinylation was achieved by addition of 2 ml of ice-cold Dulbecco's phosphate-buffered saline containing 0.5 mg/ml Sulfo-NHS-LC-Biotin (Pierce Biotechnology Inc., Rockford, IL, USA) to the apical side (filter top) and 3 ml of Dulbecco's phosphate-buffered saline containing 0.5% bovine serum albumin to the basolateral side below the filter to facilitate quenching of any biotin across the membrane. Conversely, basolateral biotinylation was achieved by reversing the position of the prescribed solutions. Biotinylation reactions were incubated for 30 min at 4°C and then terminated by twice washing cells with ice-cold quenching solution (100 mM glycine, Dulbecco's phosphate-buffered saline) followed by incubation with a third rinse of quenching solution for 20 min at 4°C.

Precipitation of biotinylated and/or His-tagged proteins

Precipitation of biotinylated proteins with SA_v-agarose (Pierce) was performed using IMCD transfectants lysed with ice-cold lysis buffer (1% Triton X-100, 50 mM Tris pH 7.5, 150 mM NaCl, 5 mM EDTA supplemented with Complete[®] Protease Inhibitor tablets). After 0.5–1 h lysates were clarified by centrifugation at $14\,000 \times g$ for 10 min, and lysates were incubated with SA_v-agarose (50–100 μ l of packed beads) for 4–16 h with agitation at 4°C. Beads were then washed twice with lysis buffer, twice with high salt wash buffer (0.1% Triton X-100, 50 mM Tris pH 7.5, 500 mM NaCl, 5 mM EDTA), and once with 10 mM Tris pH 7.5. His-tagged proteins were precipitated from IMCD transfectants lysed with Ni-NTA lysis buffer (1% Triton X-100, 0.5% deoxycholate, 50 mM NaH₂PO₄,

300 mM NaCl, 10 mM imidazole, Complete[®] protease inhibitor tablets without EDTA). Clarified lysates (following centrifugation at $14\,000 \times g$ for 10 min) were incubated with 100 μ l packed beads of Ni-NTA-agarose (Invitrogen) 4–16 h at 4°C, after which beads were washed thrice with Ni-NTA lysis buffer. Proteins were eluted from beads by addition of equal volume of $2 \times$ SDS-PAGE sample buffer followed by incubation at 100°C for 5 min.

Isolation of total membranes from kidney cortex

Snap-frozen tissue (25–50 mg) was homogenized in ice-cold $1 \times$ total membrane proteins (TMP) buffer (25 mM Tris-SO₄ pH 7.5, 150 mM NaCl, 1 mM EDTA) supplemented with protease inhibitor cocktail (One Complete[®] tablet per 25–50 ml buffer; Roche Applied Science, Penzberg, Germany) and then incubated on ice for 30 min. Cellular debris was pelleted by centrifugation at $1000 \times g$ for 10 min at 4°C. Supernatants were recovered and then total membranes were pelleted by centrifugation at $110\,000 \times g$ for 1 h at 4°C. The supernatants were decanted and pelleted membranes were resuspended in 100–200 μ l TMP buffer. Protein concentration in membrane preparations was determined by the Bio-Rad Protein Assay (Bio-Rad Laboratories, Hercules, CA, USA) using bovine serum albumin as a standard.

Fractionation of membrane vesicles isolated from kidney cortex

Basolateral membrane vesicles were enriched from rabbit kidney cortex by Percoll density fractionation as described by Grassl and Aronson.⁵² Briefly, kidney cortex (5 g) was initially homogenized with Tekmar TK10 homogenizer in $4 \times$ (weight/volume) ice-cold hepes-buffered sucrose with EDTA (HBE) (10 mM *N*-2-hydroxyethylpiperazine-*N'*-2-ethanesulphonic acid, 250 mM sucrose pH 7.6, supplemented with Complete[®] Protease Inhibitor tablets) and then Dounce homogenized (30 strokes). Homogenates were clarified by centrifugation at $2500 \times g$ for 15 min at 4°C. The supernatant was collected, and pellets were resuspended in HBE and Dounce homogenized for an additional 20 strokes and centrifuged ($2500 \times g$ for 15 min at 4°C). Supernatants were combined and membrane vesicles were pelleted by centrifugation ($20\,000 \times g$) for 20 min. Membrane vesicles (white fluffy layer) were gently resuspended from the pellet by aspiration, centrifuged ($20\,000 \times g$) for 20 min, and then resuspended in less than 1 ml of HBE. Membrane vesicles were Dounce homogenized for five strokes and 0.45 ml were layered over 13.65% Percoll[™] (Amersham Biosciences, Piscataway, NJ, USA) in HBE (8.5 ml) and centrifuged ($48\,000 \times g$) for 30 min. This fractionation separates basolateral from apical membrane vesicles. Fractions (0.5–1.0 ml) were collected from Percoll density gradients and washed with five volumes of HBE buffer and stored at -80°C until use. Total protein concentration in each fraction was determined by utilizing the BioRad protein assay reagent micro-method and a bovine serum albumin standard according to recommended protocols.

PI-PLC Digestion and Triton X-114 Partitioning

Duplicates of membrane fractions (20–100 μ g) were adjusted to 10 mM Tris-HCl, 144 mM NaCl by addition of appropriate volume of $5 \times$ reaction buffer and $\sim 1 \mu$ g of PI-PLC was added to one set of duplicates and both sets were incubated overnight at 37°C. Following digestion, the sample volume was adjusted to 100–200 μ l with ice-cold TBS and 1/5 volume of pre-condensed Triton X-114 (final $\sim 2\%$) was added, mixed by vortexing, and then

chilled on ice for 15 min with occasional mixing. Samples were warmed to 37°C and then centrifuged (1000 × g). The upper AQ (cleaved or non-GPI-linked protein) was separated from the DG containing GPI-linked or transmembrane proteins. The DG was twice back extracted with ice-cold TBS to facilitate partitioning of soluble versus membrane-anchored proteins. Proteins were precipitated from the AQ and DGs by TCA-DOC method where 1/100 volume of 2% sodium deoxycholate was added and samples were incubated on ice for 30 min followed by addition of 1/10 volume of 100% TCA and incubated at 4°C for 16 h. Samples were then centrifuged (15 000 × g) for 15 min at 4°C, and protein pellets were washed twice with cold acetone, air-dried, and solubilized in 1 × SDS-PAGE sample buffer.

Deglycosylation of CAIV

Membrane vesicles (15–25 μg total protein) prepared from kidney cortex (see above) were adjusted to 20 mM sodium phosphate, pH 7.5, 0.02% sodium azide, 0.1% SDS, 50 μM β-mercaptoethanol, and denatured by heating at 100°C for 5 min. Samples were allowed to cool to room temperature and then adjusted to 0.75% NP-40. N-glycanase (~2.5 mU) was added and reactions were incubated overnight at 37°C. Equal volume of 2 × sample buffer (100 mM Tris, pH 6.8, 20% glycerol 4% SDS, 50 μM 2-mercaptoethanol, 0.05% bromophenol blue) was added and glycanase-treated samples were again heated at 100°C for 5 min. Proteins were resolved on 10 or 12% SDS-PAGE gels and Western blotted for CAIV as described below.

SDS-PAGE and Western blotting

Proteins were resolved by SDS-PAGE (8, 10, or 12% 37.5:1 Acrylamide/bis-acrylamide; Tris-glycine), and transferred to nitrocellulose membranes (Bio-Rad) utilizing a Panther (HEP-1) semidry electroblotter (Owl Scientific, Cambridge, MA, USA) and Towbin's buffer according to recommended protocols. Membranes were then blocked with 3% casein (EMD chemicals Inc., Gibbstown, NJ, USA) in TBS supplemented with 0.05% Tween 20. Incubations with primary antibodies were carried out in heat-sealable bags with 3 ml of 1% casein TBS supplemented with 0.05% Tween 20 for 16 h at 4°C, followed by 3 × 10 min washes with TBS supplemented with 0.05% Tween 20. Incubations with HRP-conjugated secondary antibodies were carried for 2–4 h at room temperature and followed by 3 × 10 min washes with TBS supplemented with 0.05% Tween 20 and one wash in TBS. Western blots were developed with ECL™ chemiluminescent substrate (Amersham Biosciences), and chemiluminescence was detected by exposure to Hyperfilm™ (Amersham) for up to 15 min.

Microassay for quantification of CA hydratase activity in membrane fractions

The imidazole-Tris end point assay described by Brion *et al.*^{24,25} was used to quantify hydratase activity in membrane fractions. Briefly, 50 ml of reaction buffer (20 mM imidazole, 5 mM Tris, and 0.4 mM *p*-nitrophenol) were added via Hamilton syringe to an equal volume containing 10–30 μg of total membrane protein. Reactions were carried out in 6 × 50 mm glass tubes. All reagents and samples were chilled on ice, and all reactions were carried in a 0°C ice bath. The reaction was continuously bubbled with CO₂ until the solution acidified and the yellow color of *p*-nitrophenol was no longer detectable. The CO₂ flow rate was adjusted such that the time required for color change by a water control sample was between 65 and 75 s.

Enzyme activity was expressed as EU/mg protein and was determined using the following formula:

$$CA \text{ (EU/mg protein)} = \log(B/S)/(\text{prot})\log(2),$$

where *B* is the time (s) for boiled/inactive sample and *S* is the sample time. The term (prot) denotes milligrams of membrane protein in the sample and $\log 2 = 0.301$. SDS-resistant activity was determined by treating membrane samples with 1–2% SDS for 1 h at room temperature before diluting the sample to ~0.1% SDS for analysis. For two of three experiments boiled/inactive sample hydratase activity was determined by the time (s) for a color change in membrane fractions that had been heated at 100°C for 15 min; for the third experiment samples treated with 100 μM acetazolamide established the boiled/inactive baseline time. The time required for color change in boiled samples and acetazolamide-treated samples were essentially equivalent (65–75 s). The baseline values for SDS-treated samples were determined from corresponding boiled or acetazolamide-treated samples containing equivalent concentrations of SDS. SDS-resistant activity was divided by the activity with no treatment to provide a percentage of CAIV activity in apical versus basolateral fractions.

Statistics

Data are presented as mean ± s.d. Paired and unpaired *t*-tests were performed using Excel 2003 (Microsoft Corp., Bellvue, WA, USA). Significance was asserted if *P* < 0.05.

ACKNOWLEDGMENTS

This work has been supported in part by NIH Grant DK 50603 and a Grant-in-aid from the American Heart Association Northeast Affiliate (0455829T).

REFERENCES

- Schwartz GJ. Physiology and molecular biology of renal carbonic anhydrase. *J Nephrol* 2002; **15**: S61–S74.
- Schwartz GJ, Kittelberger AM, Barnhart DA, Vijayakumar S. Carbonic anhydrase IV is expressed in H⁺-secreting cells of the rabbit kidney. *Am J Physiol* 2000; **278**: F894–F904.
- Tureci O, Sahin U, Vollmar E *et al.* Human carbonic anhydrase XII: cDNA cloning, expression, and chromosomal localization of a carbonic anhydrase gene that is overexpressed in some renal cell cancers. *Proc Natl Acad Sci USA* 1998; **95**: 7608–7613.
- Kyllönen MS, Parkkila S, Rajaniemi H *et al.* Localization of carbonic anhydrase XII to the basolateral membrane of H⁺-secreting cells of mouse and rat kidney. *J Histochem Cytochem* 2003; **51**: 1217–1224.
- Parkkila S, Parkkila A-K, Saarnio J *et al.* Expression of the membrane-associated carbonic anhydrase isozyme XII in the human kidney and renal tumors. *J Histochem Cytochem* 2000; **48**: 1601–1608.
- Schwartz GJ, Kittelberger AM, Watkins RH, O'Reilly MA. Carbonic anhydrase XII mRNA encodes a hydratase that is differentially expressed along the rabbit nephron. *Am J Physiol* 2003; **284**: F399–F410.
- Halmi P, Lehtonen J, Waheed A *et al.* Expression of hypoxia-inducible, membrane-bound carbonic anhydrase isozyme XII in mouse tissues. *Anat Rec Part A* 2004; **277A**: 171–177.
- Mori K, Ogawa Y, Ebihara K *et al.* Isolation and characterization of CA XIV, a novel membrane-bound carbonic anhydrase from mouse kidney. *J Biol Chem* 1999; **274**: 15701–15705.
- Kaunisto K, Parkkila S, Rajaniemi H *et al.* Carbonic anhydrase XIV: luminal expression suggests key role in renal acidification. *Kidney Int* 2002; **61**: 2111–2118.
- Lucci MS, Tinker JP, Weiner IM, DuBose Jr TD. Function of proximal tubule carbonic anhydrase defined by selective inhibition. *Am J Physiol* 1983; **245**: F443–F449.
- Tsuruoka S, Schwartz GJ. HCO₃⁻ absorption in rabbit outer medullary collecting duct: role of luminal carbonic anhydrase. *Am J Physiol* 1998; **274**: F139–F147.

12. Brechue WF, Kinne-Saffran E, Kinne RKH, Maren TH. Localization and activity of renal carbonic anhydrase (CA) in CA-II deficient mice. *Biochim Biophys Acta* 1991; **1066**: 201–207.
13. Sly WS, Whyte MP, Krupin T, Sundaram V. Positive renal response to intravenous acetazolamide in patients with carbonic anhydrase II deficiency. *Pediatr Res* 1985; **19**: 1033–1036.
14. Zhu XL, Sly WS. Carbonic anhydrase IV from human lung: purification, characterization, and comparison with membrane carbonic anhydrase from human kidney. *J Biol Chem* 1990; **265**: 8795–8801.
15. Waheed A, Zhu XL, Sly WS. Membrane-associated carbonic anhydrase from rat lung: purification, characterization, tissue distribution, and comparison with carbonic anhydrase IVs of other mammals. *J Biol Chem* 1992; **267**: 3308–3311.
16. Powell SK, Cunningham BA, Edelman GM, Rodriguez-Boulan E. Targeting of transmembrane and GPI-anchored forms of N-CAM to opposite domains of a polarized epithelial cell. *Nature* 1991; **353**: 76–77.
17. Lonnerholm G, Wistrand PJ. Membrane-bound carbonic anhydrase CA IV in the human kidney. *Acta Physiol Scand* 1991; **141**: 231–234.
18. Brown D, Zhu XL, Sly WS. Localization of membrane-associated carbonic anhydrase type IV in kidney epithelial cells. *Proc Natl Acad Sci USA* 1990; **87**: 7457–7461.
19. Tsuruoka S, Swenson ER, Petrovic S *et al*. Role of basolateral carbonic anhydrase in proximal tubular fluid and bicarbonate absorption. *Am J Physiol* 2001; **280**: F146–F154.
20. Winkler CA, Kittelberger AM, Schwartz GJ. Expression of carbonic anhydrase IV mRNA in rabbit kidney: stimulation by metabolic acidosis. *Am J Physiol* 1997; **272**: F551–F560.
21. Low MG. Glycosyl-phosphatidylinositol: a versatile anchor for cell surface proteins. *FASEB J* 1989; **3**: 1600–1608.
22. Okuyama T, Sato S, Zhu XL *et al*. Human carbonic anhydrase IV: cDNA cloning, sequence comparison, and expression in COS cell membranes. *Proc Natl Acad Sci USA* 1992; **89**: 1315–1319.
23. Whittington DA, Grubbs JH, Waheed A *et al*. Expression, assay, and structure of the extracellular domain of murine carbonic anhydrase XIV. *J Biol Chem* 2004; **279**: 7223–7228.
24. Brion LP, Schwartz JH, Zamilowitz BJ, Schwartz GJ. Micro-method for the measurement of carbonic anhydrase activity in cellular homogenates. *Anal Biochem* 1988; **175**: 289–297.
25. Brion LP, Zamilowitz BJ, Suarez C, Schwartz GJ. Metabolic acidosis stimulates carbonic anhydrase activity in rabbit proximal tubule and medullary collecting duct. *Am J Physiol* 1994; **266**: F185–F195.
26. McGwire GB, Becker RP, Skidgel RA. Carboxypeptidase M, a glycosylphosphatidylinositol-anchored protein, is localized on both the apical and basolateral domains of polarized Madin–Darby canine kidney cells. *J Biol Chem* 1999; **274**: 31632–31640.
27. Sarnataro D, Paladino S, Campana V *et al*. PrP^C is sorted to the basolateral membrane of epithelial cells independently of its association with rafts. *Traffic* 2002; **3**: 810–821.
28. Zurzolo C, Lisanti MP, Caras IW *et al*. Glycosylphosphatidylinositol-anchored proteins are preferentially targeted to the basolateral surface in Fischer rat thyroid epithelial cells. *J Cell Biol* 1993; **121**: 1031–1039.
29. Selvaggio AM, Schwartz JH, Bengel HH *et al*. Mechanisms of H⁺ secretion by inner medullary collecting duct cells. *Am J Physiol* 1988; **254**: F391–F400.
30. Rodriguez-Boulan E, Musch A. Protein sorting in the Golgi complex: shifting paradigms. *Biochim Biophys Acta* 2005; **1744**: 455–464.
31. Udenfriend S, Kodukula K. How glycosylphosphatidylinositol-anchored proteins are made. *Ann Rev Biochem* 1995; **64**: 563–591.
32. Low MG. The glycosyl-phosphatidylinositol anchor of membrane proteins. *Biochim Biophys Acta* 1989; **988**: 427–454.
33. Fanjul M, Alvarez L, Salvador C *et al*. Evidence for a membrane carbonic anhydrase IV anchored by its C-terminal peptide in normal human pancreatic ductal cells. *Histochem Cell Biol* 2004; **121**: 91–99.
34. Okuyama T, Waheed A, Kusumoto W *et al*. Carbonic anhydrase IV: role of removal of C-terminal domain in glycosylphosphatidylinositol anchoring and realization of enzyme activity. *Arch Biochem Biophys* 1995; **320**: 315–322.
35. Brown DA, Rose JK. Sorting of GPI-anchored proteins to glycolipid-enriched membrane subdomains during transport to the apical cell surface. *Cell* 1992; **68**: 533–544.
36. Brown D, Waneck GL. Glycosyl-phosphatidylinositol-anchored membrane proteins. *J Am Soc Nephrol* 1992; **3**: 895–906.
37. Hooper NM, Bashir A. Glycosyl-phosphatidylinositol-anchored membrane proteins can be distinguished from transmembrane polypeptide-anchored proteins by differential solubilization and temperature-induced phase separation in Triton X-114. *Biochem J* 1991; **280**: 745–751.
38. Hooper NM, Turner AJ. Ecto-enzymes of the kidney microvillar membrane. Differential solubilization by detergents can predict a glycosyl-phosphatidylinositol membrane anchor. *Biochem J* 1988; **250**: 865–869.
39. Arreaza G, Brown DA. Sorting and intracellular trafficking of a glycosylphosphatidylinositol-anchored protein and two hybrid transmembrane proteins with the same ectodomain in Madin–Darby canine kidney epithelial cells. *J Biol Chem* 1995; **270**: 23641–23647.
40. Sharma P, Sabharanjak S, Mayor S. Endocytosis of lipid rafts: an identity crisis. *Cell Dev Biol* 2002; **13**: 205–214.
41. Slimane TA, Trugnan G, van IJendoorn SC, Hoekstra D. Raft-mediated trafficking of apical resident proteins occurs in both direct and transcytotic pathways in polarized hepatic cells: role of distinct lipid microdomains. *Mol Biol Cell* 2003; **14**: 611–624.
42. Pang S, Urquhart P, Hooper NM. N-glycans, not the GPI anchor, mediate the apical targeting of a naturally glycosylated, GPI-anchored protein in polarised epithelial cells. *J Cell Sci* 2004; **117**: 5079–5086.
43. Sarnataro D, Nitsch L, Hunziker W, Zurzolo C. Detergent insoluble microdomains are not involved in transcytosis of polymeric Ig receptor in FRT and MDCK cells. *Traffic* 2000; **1**: 794–802.
44. Benting JH, Rietveld AG, Simons K. N-glycans mediate the apical sorting of a GPI-anchored, raft-associated protein in Madin–Darby canine kidney cells. *J Cell Biol* 1999; **146**: 313–320.
45. Paladino S, Sarnataro D, Pillich R *et al*. Protein oligomerization modulates raft partitioning and apical sorting of GPI-anchored proteins. *J Cell Biol* 2004; **167**: 699–709.
46. Schuck S, Simons K. Polarized sorting in epithelial cells: raft clustering and the biogenesis of the apical membrane. *J Cell Sci* 2004; **117**: 5955–5964.
47. Schell MJ, Maurice M, Stieger B, Hubbard AL. 5' Nucleotidase is sorted to the apical domain of hepatocytes via an indirect route. *J Cell Biol* 1992; **119**: 1173–1182.
48. Polishchuk R, DiPentima A, Lippincott-Schwartz J. Delivery of raft-associated, GPI-anchored proteins to the apical surface of polarized MDCK cells by a transcytotic pathway. *Nat Cell Biol* 2004; **6**: 297–307.
49. Gross E, Kurtz I. Structural determinants and significance of regulation of electrogenic Na⁺-HCO₃⁻ cotransporter stoichiometry. *Am J Physiol* 2002; **283**: F876–F887.
50. Alvarez BV, Loisel FB, Supuran CT *et al*. Direct extracellular interaction between carbonic anhydrase IV and the human NBC1sodium/bicarbonate co-transporter. *Biochemistry* 2003; **42**: 12321–12329.
51. Ojakian GK, Schwimmer R. The polarized distribution of an apical cell surface glycoprotein is maintained by interactions with the cytoskeleton of Madin–Darby canine kidney cells. *J Cell Biol* 1988; **107**: 2377–2387.
52. Grassl SM, Aronson PS. Na⁺/HCO₃⁻ co-transport in basolateral membrane vesicles isolated from rabbit renal cortex. *J Biol Chem* 1986; **261**: 8778–8783.